Chemical Engineering Journal 425 (2021) 130656

Contents lists available at ScienceDirect

Chemical Engineering Journal

journal homepage: www.elsevier.com/locate/cej

3D printed reactor-in-a-centrifuge (RIAC): Making flow-synthesis of nanoparticles pump-free and cost-effective

Domenico Andrea Cristaldi [a,b,*], Alessio Labanca [a], Tomas Donal Pottinger [b], Joshua Owen [c], Eugen Stulz [b,d], Xunli Zhang [a,d], Dario Carugo [e,*]

[a] Faculty of Engineering and Physical Sciences (FEPS), University of Southampton, Highfield, Southampton SO17 1BJ, UK
[b] School of Chemistry, University of Southampton, Highfield, Southampton SO17 1BJ, UK
[c] Center for Clinical Research, National Institutes of Health, Bethesda, MD 20892, United States
[d] Institute for Life Sciences (IfIS), University of Southampton, Highfield, Southampton SO17 1BJ, UK
[e] Department of Pharmaceutics, UCL School of Pharmacy, University College London, London WC1E 6BT, UK

ARTICLE INFO

Keywords:
Liposomes
Silver nanoparticles
3D printing
Flow-reactors
Centrifuge
Rapid prototyping

ABSTRACT

It is widely recognised that flow-reactors offer greater control over the stoichiometry of chemical reactions when compared to batch methods, since they provide finer and more predictable regulation over the transport of fluids and chemical species. These characteristics are of critical importance in the context of nanoparticle production, since the physical and chemical properties of the fluidic environment within a reactor strongly influence the size and/or shape of the end-product. In the past decade, replica moulding techniques (e.g., based on soft-lithography) have been developed to manufacture flow-reactors in a relatively cost-effective and efficient fashion. However, devices are often operated using multiple syringe pumps, and several of these techniques require laborious and multi-step procedures. In this study, we developed rapidly prototyped reactors embedded within a cylindrical structure that are designed for actuation using a laboratory centrifuge (herein referred to as reactor-in-a-centrifuge, or RIAC). Using RIACs of different architecture, we demonstrated production of nano-scale liposomes of therapeutically relevant size (in the diameter range 80 – 300 nm) under varying operating conditions. We also demonstrated production of silver nanospheres (with UV–vis absorption maxima of 404 nm) at selected operating conditions. The novel concept proposed in this study has the potential to significantly simplify the synthesis of nanomaterials over more commonly used microfluidic techniques, as it relies on a cost-effective and single-step reactor manufacturing process (using a desktop 3D printer) and employs widely available laboratory centrifuges to drive reagents through the reactor. In this paper we describe RIAC's design, manufacturing, and actuation protocols, and demonstrate its applicability to the flow synthesis of nanoparticles without relying on highly specialised instrumentation or costly procedures.

1. Introduction

Chemical reactors that carry materials in a flowing stream (often referred to as 'flow reactors') exhibit unique characteristics over their batch counterparts, since they provide enhanced stoichiometric control and increased production yield, while reducing waste of expensive or hazardous chemicals [1]. The manufacturing of miniaturised flow reactors however, often involves the use of expensive materials and laborious protocols, and is frequently performed under environmentally controlled conditions within highly specialised facilities (i.e. clean-rooms) [2]. Over the last two decades, numerous chemical syntheses have been performed using nano-, micro- and milli-fluidic channel architectures [3]. In particular, a multitude of flow-reactor configurations have been designed for the production of both organic vesicles [4,5] and inorganic nanomaterials [6]. The scalability of manufacturing processes for these reactors has significantly improved with the advent of soft-lithography [7], in which multiple replica of a device can be fabricated from a single master mould. With soft-lithography, silicone elastomers (such as polydimethylsiloxane, PDMS) are commonly used as the constitutive material of the channel replica [2]. Recently, three-dimensional (3D) printing has emerged as a cost-effective and robust technology to either fabricate flow reactors in a single step [8,9], or to

* Corresponding authors at: Department of Pharmaceutics, UCL School of Pharmacy, University College London, London WC1E 6BT, UK (D. Carugo).
E-mail addresses: d.a.cristaldi@soton.ac.uk (D. Andrea Cristaldi), d.carugo@ucl.ac.uk (D. Carugo).

https://doi.org/10.1016/j.cej.2021.130656
Received 28 September 2020; Received in revised form 24 May 2021; Accepted 30 May 2021
Available online 4 June 2021

generate master moulds for soft-lithography [10]. Nevertheless, expensive or customizable 3D printers are generally required to accurately manufacture moulds containing micrometre-sized features [11]. Moreover, the PDMS channel replica fabricated *via* soft-lithography require sealing to a substrate (typically glass or PDMS), which is often achieved by surface activation with oxygen plasma [10,12]. The need for sophisticated instrumentation has thus often limited the scalability of microfluidic-based flow reactor technologies, hindering their industrial translation or adoption by low-resource research laboratories. To overcome this limitation, we recently developed a cost-effective and facile manufacturing process (~£5 per device, fabrication time < 24 h), involving 3D printed master moulds made using desktop 3D printers to generate PDMS channel replica, which were then manually sealed to a pressure-sensitive adhesive tape [13].

In addition to the type of manufacturing process however, the operational costs and scalability of flow reactors also depend on the type of fluid dispensing system used to deliver reagents. The majority of microfluidic devices are operated using expensive and bulky syringe pumps, which can limit the simultaneous operation of multiple reactors [14]. To avoid the use of syringe pumps, alternative technologies have been developed, including the so-called lab-on-a-CD (or lab-on-a-disk, LoaD) concept, in which microfluidic channels are incorporated within a Compact Disc (CD) sized substrate [15]. The spinning motion of the disk generates three main forces (centrifugal, Euler, and Coriolis), which can be tuned to deliver reagents through the channels at controlled rates [16]. Although LoaDs containing branched channel architectures are suitable for complex applications, such as microarray processing [17], only small fluid volumes can be processed with this method and the associated manufacturing techniques are significantly more complex when compared to rapid prototyping.

The use of centrifugal forces to enhance automation of DNA extraction from whole blood samples and purification of His-tagged proteins has been demonstrated by Kloke *et al.*, using the so-called LabTube devices [18]. Similar devices have also been employed for the detection of foodborne microorganisms [19]. Due to their complex architecture, LabTube cartridges require multiple manufacturing procedures, often including injection moulding, LED scanning, stereolithography, and thermal sealing. Nonetheless, due to its simplicity of usage, the latter method inspired the present study.

Herein, we present an easy-to-use and pump-free technology actuated by an ordinary centrifuge, that only relies on the use of a 3D printed flow-through reactor (referred to as reactor-in-a-centrifuge, or RIAC). In this manuscript, we describe iterative developments of RIAC's design and manufacturing process, as well as demonstrate its applicability to the production of both organic and inorganic nanoparticulate systems, namely liposomes and silver nanospheres. The former find widespread applications in drug delivery for cancerous and infectious disease treatment [20], while the latter are employed in many other fields ranging from anti-bacterial to anti-inflammatory therapies and imaging [21].

To the best of the authors' knowledge, this is the first study reporting on the manufacturing of both organic and inorganic nanoparticulate systems using a centrifuge-actuated flow-reactor. It is anticipated that the reactor design proposed in this study has the potential to be scaled-up in future work by operating multiple rigs simultaneously, without the need for sophisticated control units or sensors, and that production continuity could be enhanced by automating the processes of reactor's priming and end-product collection. Depending on the required application, temperature-controlled and continuous-flow centrifuges may also be employed, both of which are commercially available or could be custom-made. To facilitate the replication and adoption of the device by different laboratories, in addition to the description below, RIAC technical drawings (in *.stl* format) are provided as supplementary material to this manuscript.

2. Materials and methods

2.1. Reactor-in-a-centrifuge (RIAC): Design rationale and specifications

RIACs were designed using a CAD software (Solidworks®), and 3D printed in polylactic acid (PLA) *via* a fused deposition modelling (FDM) printer (Ultimaker 2+). The device architecture comprises two equally sized reservoirs connected to a mixing channel through a Y-junction. Both reservoirs and channels are embedded within a cylindrical body, which is designed to be hosted in a standard 50 mL centrifuge tube. After testing various prototypes, two different geometries of the mixing channel were evaluated and compared: straight (channel inner radius: 0.75 mm, channel length: 51 mm) and spiral (channel inner radius: 1.00 mm, radius of curvature: 6.5 mm, channel length: 102 mm, number of revolutions: 2) (see Fig. 1A and 1B, respectively). Technical drawings are also provided as supplementary material to this manuscript.

In both cases, RIAC's design was conceived to avoid the printing of supporting material inside both channels and reservoirs. A single-body and a two-components configuration (comprising body and bottom support) were adopted for the straight- and spiral-RIAC, respectively (Fig. 1A and B). The two-component configuration for the spiral-RIAC was created to avoid the presence of supporting material at the bottom surface of the reservoirs or within the channels, as described in the following paragraph.

An additional challenge was to prevent reagents from flowing through the device before actuation. Initially, a layer of filter paper or sponge was placed on the bottom surface of the reservoirs, but their performance was not deemed satisfactory. A new design was thus subsequently developed, which could host high performance liquid chromatography (HPLC) frit filters into a recess (Fig. 1B and F). These filters are often made of compacted metal microspheres with interstices (or pores) between them, the size of which depends on the sphere diameter and compaction pressure applied during manufacturing. As for other applications of these filters, it is anticipated that the they will allow retainment of fluids in the RIAC reservoirs upon priming due to the high hydraulic resistance offered and liquid's surface tension, and that liquids will subsequently flow through the interstices under the action of centrifugal forces. Given the small pore size (in the order of 0.5 – 2.0 μm), laminar flow conditions through the filter are typically assumed [22]. The presence of frit filters also enables separation of unconsumed reactants (retained within the reservoirs) from the end-product (located at the bottom of the centrifuge tube), in the case of incomplete reactants consumption.

Devices could be operated at relative centrifugal force (rcf) in the 28 – 1′789 range, with no detectable leakage through the frit seats or the body of the device. The lowest rcf corresponded to the minimum centrifugal force required to drive fluids through the frit filters (with 2 mL of fluid in each reservoir). A structural integrity test was also performed, demonstrating successful operation without mechanical damage until a maximum rcf value of 13′528.

2.2. RIAC manufacturing: 3D printer settings

As described above, the channel architecture was manufactured within a cylindrical scaffold using an FDM printer, for integration into conventional centrifuge tubes. The CURA software (version 15.04.6) was used to define the characteristics of the 3D printing process, and the following settings were adopted: layer height = 0.1 mm, bottom/top thickness = 0.5 mm, infill density = 100%, infill patterns = lines, print speed = 50 mm/s, and nozzle size = 0.4 mm. Using these printing settings, the total amount of PLA required to manufacture one device was of 29 g.

Fused deposition modelling 3D printers, similarly to other 3D printing methods, require supporting material when manufacturing certain architectures. This typically occurs when the design comprises of a roof that would collapse if not adequately supported, or when specific

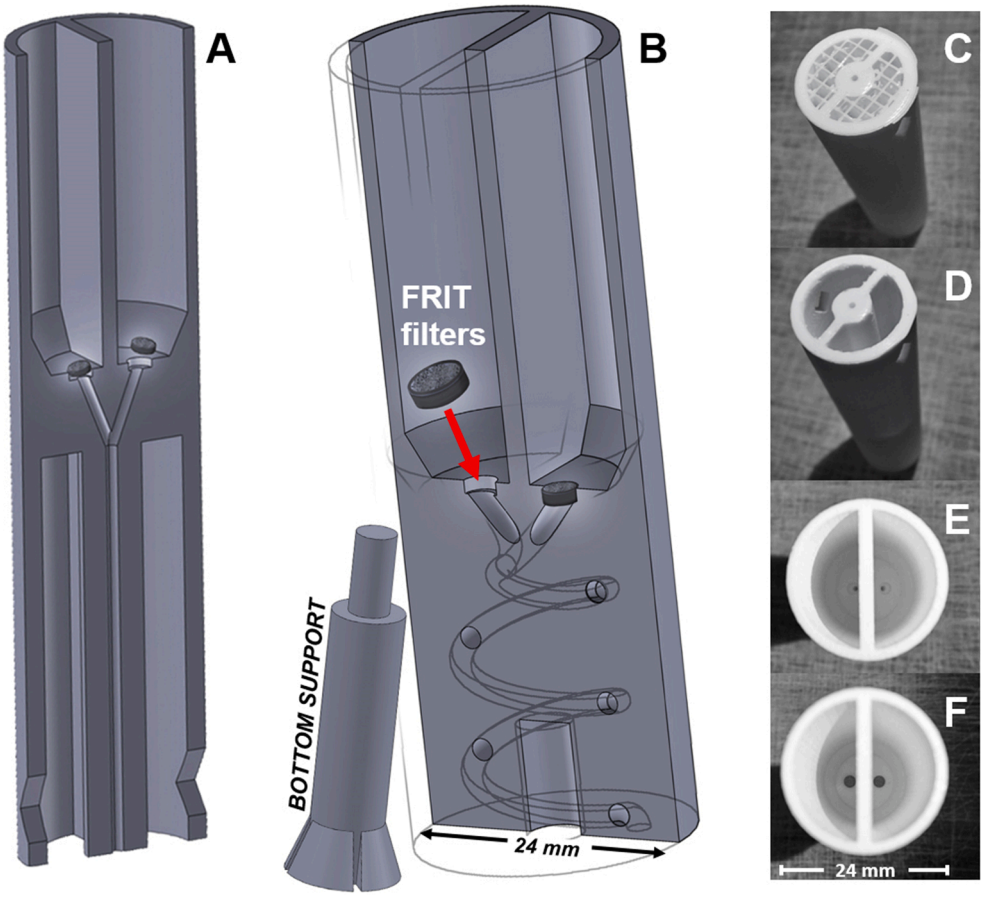

Fig. 1. Cross-sectional CAD drawings of RIACs, having either straight (A) or spiral (B) mixing channels. Frit filters (3.175 mm in diameter) are inserted into a recess at the bottom of the reservoirs, as indicated by the red arrow. The bottom support (B) is designed for the spiral-RIAC to allow sample collection from the centrifuge tube. Photograph of the 3D printed RIAC-straight channel, before (C) and after (D) removing the supporting material. A top view of the device in the absence (E) and presence (F) of frit filters is also shown.

design features (such as inclined surfaces) exceed the printable angle limit. Consequently, when manufacturing the RIAC, particular attention was given to the architecture and spatial orientation of the reactor.

The straight-channel RIAC was printed in a single piece, by designing a bottom chamber that provided structural support to the device, and also facilitated collection of the end-product. On the other hand, the spiral-RIAC required additional design features to overcome 3D printing limitations. The adopted final design (Fig. 1B, and supplementary technical drawings) consisted of two separate pieces (i.e., main body and bottom support), which were first printed individually and then connected to each other.

During the printing process, reservoirs were kept upward to avoid the creation of supporting material inside them (Fig. 2). This allowed accurate construction of the bottom surfaces of both reservoirs and frit seats, and importantly it did not require post-fabrication treatments. By adopting this device orientation, the supporting material was printed only within the hole used for connecting the bottom support to the main body (Fig. 2B). This material did not interfere with the mixing channel architecture and could be easily removed. Importantly, by prototyping an accurate rounded geometry within the angle limit of the 3D printer,

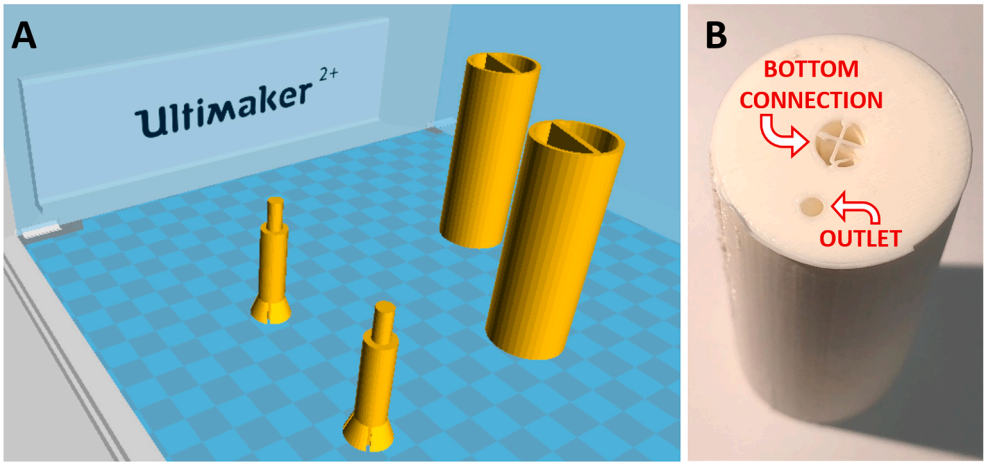

Fig. 2. (A) Orientation of the spiral-RIAC and its bottom support element for the 3D printing manufacturing process. The image is captured from the 3D printer software (CURA). (B) Bottom surface of the spiral-RIAC showing the mixing channel outlet and the hole for connection between the main RIAC's body and the bottom support.

no supporting material was generated at the outlet of the mixing channel (Fig. 2B) and within the mixing channel itself.

2.3. Liposome production: chemicals and sample preparation

Liposomes were prepared using phosphatydilcoline (PC) (Lipoid GmbH, Germany) and dimethyldioctadecylammonium bromide 98% (DDAB) (Sigma-Aldrich Co., USA). Ethanol absolute was purchased from Fisher Scientific Ltd. (UK), while Milli-Q water was supplied through the QGard purification filter connected to the Milli-Q Gradient A10 system (Merck Millipore, USA). The desired concentration of a stock solution of PC:DDAB (9:1 M ratio) was obtained by weighing the required amount of each compound and dissolving it in ethanol. The obtained solution was then filtered using a 0.20 μm pore size Millex®-GN syringe filter (Merck Millipore Ltd., UK).

For producing liposomes, a solvent exchange mechanism frequently used in microfluidic-based methods [23], was adopted to identify suitable synthesis conditions. This method relies on the mixing between an organic solvent in which lipids are solubilised (in this case ethanol) and a non-solvent (typically water), leading to the self-assembly of lipids to form vesicular systems. It has been postulated that when the phospholipid molecules encounter an aqueous environment, they spontaneously arrange into a planar bilayer in order to minimize unfavourable interactions between the hydrophobic acyl chain of the molecules and the aqueous phase. Subsequently, the formed planar bilayers enclose to form a vesicular architecture [24].

For the production of liposomes, 2 mL of milli-Q water were pipetted into one reservoir and 2 mL of the ethanolic lipid solution (containing a selected PC:DDAB concentration) into the other reservoir. An additional 6 mL of water were added at the bottom of the centrifuge tube where the RIAC was hosted. The effect of varying parameters on liposome size was investigated, including PC concentration (in the range 20–80 mM), relative centrifugal force (in the range 447–1789 rcf), and frit pore size (0.5 μm *vs.* 2.0 μm). Two different RIAC configurations were also compared, having either a straight or spiral shaped mixing channel. All experiments were conducted at room temperature (~21 °C), which is consistent with previous studies investigating flow synthesis of comparable liposome formulations [13,25].

2.4. Liposome characterization techniques

Dynamic light scattering (DLS) measurements were performed in order to determine liposome size (mean diameter) and size dispersity, using the Zetasizer Nano ZS instrument (Malvern Instrument Ltd., UK). For each sample, 1 mL of liposome suspension was transferred into a disposable Fisherbrand™ polystyrene cuvette (Fisher Scientific Ltd., UK). Prior to the measurement, samples were left into the machine for 120 s (in order to reach a temperature of 21 °C). Each sample was measured over three runs, and up to twelve scans were performed for each run. The average liposome size (expressed in terms of Z-average) and size dispersity (expressed in terms of polydispersity index, or PDI) were obtained from the Zetasizer software (Malvern Instrument Ltd, U. K., version 7.12), by averaging results obtained over four samples of the same batch (refractive index = 1.33, absorption coefficient = 0).

Liposome imaging was performed by transmission electron microscopy (TEM). An aliquot of the liposome dispersion (10 μL) was placed on a 200-mesh Formvar-coated copper grid (Agar Scientific, Stansted, Essex) and allowed to air-dry. The sample was then negatively stained with 2% w/v uranyl acetate, and allowed to air dry. A Tecnai TEM machine (T12, FEI, Hillsboro, OR) was used for image acquisition.

2.5. Spherical silver nanoparticles (AgNPs): chemicals and sample preparation

Silver nitrate 99.9999% ($AgNO_3$), tri sodium citrate dihydrate ≥ 99.0% (TSCD), polyvinylpyrrolidone (PVP), and sodium borohydride 99% ($NaBH_4$), were purchased from Sigma Aldrich UK (Gillingham, UK) and employed for the synthesis of AgNPs.

Silver nanoparticles were produced by modifying a reducing agent-based method previously employed for flow-synthesis [13]. The following solutions were initially prepared: (i) a silver source solution (SSS), comprising 20 mL of milli-Q water containing $AgNO_3$ (1.78 mM), TSCD (26.80 mM) and PVP (0.78 mM); (ii) a reducing agent solution (RAS), comprising 20 mL of milli-Q water containing $NaBH_4$ (1.33 mM); and (iii) a centrifuge tube solution (CTS), comprising 20 mL of milli-Q water containing TSCD (26.80 mM) and PVP (0.78 mM). For the synthetic protocol, one reservoir of the RIAC was filled with 2 mL of SSS while the other reservoir was filled with 2 mL of RAS. To improve NP stabilisation, 2 mL of the CTS solution were added at the bottom of the centrifuge tube. The centrifuge was operated for 2 min at 1789 rcf, and frit filters had a pore size of 0.5 μm. All experiments were conducted at room temperature (~21 °C), which is consistent with previous studies investigating flow synthesis of comparable nanoparticle formulations [13,26].

2.6. Spherical silver nanoparticles (AgNPs): Characterisation techniques

Due to their characteristic surface plasmon resonance absorption band, silver nanospheres where characterised *via* UV–visible spectroscopy, using a Varian Cary300Bio, within a 200–800 nm range with an increment step of 0.5 nm and a scanning rate of 200 nm/s. UV–vis characterisation was performed on a 1/3 (v/v) diluted sample, after gentle sonication.

Moreover, transmission electron microscopy (TEM) imaging was performed to consolidate the spectrophotometric results. Samples were prepared by drop-casting of the colloidal synthesis solution (5 μL), on carbon and Formvar coated Cu/Pd 200 mesh grids, and left to dry under atmospheric conditions at room temperature in low light. TEM images of AgNPs were acquired using the Hitachi HT7700 on the same sample used for the UV characterisation, after 1/3 further dilution.

2.7. Centrifugation settings

Relative centrifugal force (rcf) values were calculated from the revolution per minute (rpm) values, considering a centrifuge rotor's radius of 10 cm. For all experiments, RIACs were positioned always in the same orientation into an Eppendorf centrifuge 5804, where the centrifugal force drove fluids through the mixing channel. Reservoirs were labelled in order to use the assigned solvent only.

3. Results and discussion

3.1. Liposome production: identification of a suitable production protocol and formulation

In order to identify a suitable liposome production protocol, different parameters were initially evaluated, including the lipid formulation and concentration, the volume of fluids in the inlet reservoirs, the volume of water at the bottom of the centrifuge tube, the centrifugation time and relative centrifugal force (rcf) (see supplementary information, SI. 1). From these preliminary tests, it was firstly decided to use phosphatydilcoline (PC) and 10% (v/v) dimethyldioctadecylammonium bromide (DDAB) as a model lipid formulation, as it resulted in the formation of liposomes with lower mean diameter (SI. 1A, formulations 3, 4 and 6) when compared to liposomes comprising PC only (SI. 1A, formulations 1 and 2) or a mixture of PC and cholesterol (SI. 1A, formulation 5). These observations are consistent with previous studies that investigated liposome production using microfluidic-based flow reactors [23].

It was also decided to adopt a two-step production procedure as described below. Liposomal samples were prepared by adding milli-Q water into one reservoir and the ethanolic solution of PC:DDAB into the other reservoir, followed by an additional amount of water at the

bottom of the centrifuge tube. The latter not only diminished the ethanol concentration in the final liposomal suspension, but also resulted in significantly reduced liposome size and dispersity (see SI. 1B, formulations 11–14 compared to SI. 1A, formulations 3, 4 and 6). Using a dilution volume of 6 mL led to liposomes with a diameter < 300 nm (PDI < 0.4), as shown in Figure SI. 1B (formulations 11–14). A greater dilution volume (9 mL) resulted in a further slight reduction in liposome diameter and dispersity (see SI. 1B, formulation 15 *vs.* 11). However, it should be noted that an excessive dilution would decrease liposome concentration in the end-product, and therefore a compromise between desired liposome size and concentration should be considered carefully. Based on these findings, it is hypothesised that liposomes formed within the RIAC's mixing channel due to rapid mixing between ethanol and water (first step), and were subsequently conveyed into the additional volume of water located at the bottom of the centrifuge tube (second step). The resulting liposome dilution may have mitigated the detrimental effects of high centrifugal forces, which could cause liposome aggregation or rupture and thus compromise the method's reproducibility and tunability.

As a result of the preliminary tests shown in SI. 1, a most suitable formulation protocol was identified as follows: (i) 6 mL of DI water were added to the centrifuge tube, (ii) 2 mL of water and lipid ethanolic solution were separately added to the inlet reservoirs, and (iii) PC:DDAB (at 9:1 M ratio) was selected as the preferred liposome formulation.

This initial phase of the study also aimed at identifying a combination of operational parameters (i.e., centrifugal force, centrifugation time, and volume of fluid in the reservoirs) that enabled complete emptying of both reservoirs in the shortest time window (i.e., to maximise production efficiency), while still preserving the physical integrity of the reactor and producing liposomes of appropriate dimensional characteristics. It was found that a centrifugation of 2 min at ≥ 444 rcf allowed complete emptying of each reservoir filled with 2 mL of fluid, and produced liposomes with mean diameter in the therapeutically relevant range 100 – 300 nm (see SI. 1B, formulations 11–15). These operating conditions were therefore selected for subsequent experiments. Using these settings, it can be estimated that the residence time of chemical species within the RIAC was ≤ 2.70 sec and ≤ 9.61 sec for the straight- and spiral-RIAC, respectively. These values were calculated considering an average volumetric flow rate of ≥ 2 mL/min in the mixing channel (i.e., a total fluid volume of 4 mL is ejected from the RIAC in 2 min, at 444 rcf) and values of cross-sectional area and length of the mixing channel in both RIAC configurations. Notably, the estimated residence time is comparable to the one reported in previous studies that investigated production of liposomes by solvent exchange mechanism, using microfluidic-based hydrodynamic focusing devices [27].

3.2. *Liposome production: effect of lipid concentration and centrifugation parameters using both straight- and spiral-RIAC*

Different physical parameters were varied to investigate size-controlled production of liposomes using RIACs, including the initial concentration of lipid and stabilizer, relative centrifugal force (range: 447–1789 rcf), and frit pore size (0.5 and 2.0 μm). These experiments were carried out using both RIAC configurations (straight *vs.* spiral), for comparison between the two types of devices.

The results reported in Fig. 3A and 3B show that the two RIAC types generated liposomes with notable differences in their average size, over the range of lipid (PC) concentrations investigated (20–80 mM, at a fixed PC:DDAB molar ratio of 9:1). Although the straight-RIAC produced liposomes having a lower mean diameter overall, liposome size dispersity was consistently greater compared to liposomes produced using the spiral-RIAC (Fig. 3B). This could be potentially attributed to the lower estimated residence time of chemical species and mixing efficiency of the straight-RIAC compared to the spiral-RIAC, whereby complete mixing between ethanol and water may not be fully achieved within the RIAC's mixing channel.

In contrast, liposomes obtained using the spiral-RIAC had

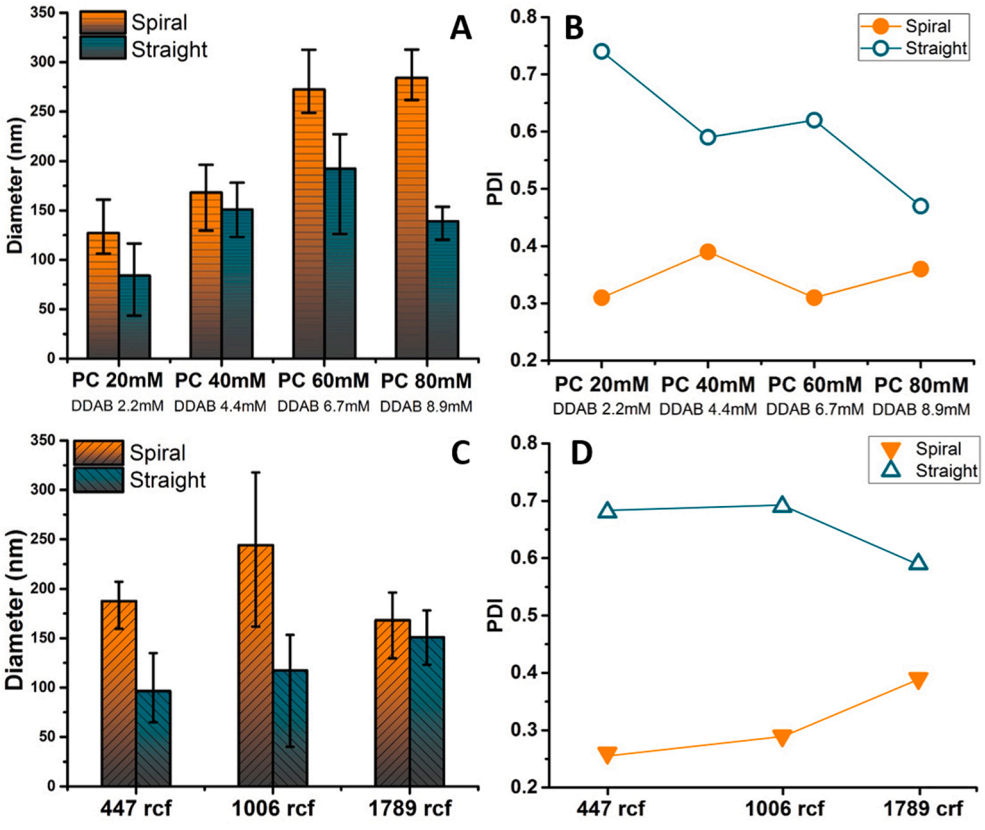

Fig. 3. Average liposome diameter (including max–min values over four independent repeats), and average PDI for the spiral *vs.* straight RIACs (frit pore size: 2.0 μm). (A) Comparison of four different initial PC:DDAB concentrations (PC concentration range: 20–80 mM, 9:1 M ratio with DDAB) with RIACs operated at 1798 rcf for 2 min, and (B) the respective PDI. (C) Effect of the g-force (range: 447–1789 rcf) on liposome diameter, for the selected PC:DDAB (40:4.4 mM) formulation, and (D) the respective PDI values.

significantly lower size dispersity, likely due to the greater estimated residence time compared to the straight-RIAC and the rapid advective mixing between ethanol and water within its curved channels. The latter could be attributed to the onset of curvature-induced secondary flows (also known as Dean flows), which originate from the generation of a pressure gradient resulting from the effect of centrifugal forces. These flows are superimposed to the primary flow, and take the form of vortices directed from the channel centre towards the wall and back towards the centre [28]. Depending on several parameters, including the channel cross-sectional area and radius of curvature, fluid's mean velocity and physical properties (i.e., density and viscosity), either one or multiple pairs of Dean vortices can form [28]. It has been previously reported that Dean flows can significantly enhance mixing of chemical species that are co-injected within helical or spiral microfluidic devices [29,30], and this has also been employed as a strategy to accelerate solvent exchange and increase production rates of liposomes in these devices. Liposomal formulations previously produced with this method encompass those reported in the present study [25,31]. It can therefore be assumed that the combined effect of enhanced mixing and greater residence time of chemical species within the spiral-RIAC both contributed to the observed reduction in liposome size dispersity compared to the straight-RIAC. In the latter, incomplete mixing within the reactor may have caused liposome formation to continue within the liquid volume at the bottom of the centrifuge tube, under less controlled mixing conditions, which may have negatively impacted on liposome size dispersity.

Furthermore, the spiral-RIAC provided adequate control over liposome diameter (from 100 to 200 nm to 250–325 nm) with increasing the initial lipid concentration (from 20 to 40 mM to 60–80 mM) (Fig. 3A), which is consistent with earlier investigations using the controlled ethanol-injection method of liposome production [23]. It should be noted that a direct comparison between the two RIAC devices does not allow elucidating the effect of a specific geometrical feature of the reactor, as the two channel architectures differ in several of their geometrical properties. It instead represents a comparative evaluation between two different types of RIAC configurations that could be manufactured using a desktop 3D printer, taking into consideration that different geometries present specific design and manufacturing constraints that determine the overall device architecture (as described in paragraph 2.1).

Although liposomes produced from PC:DDAB at 20:2.2 mM had the lowest diameter and dispersity, a more in-depth analysis of their size distribution revealed the presence of multiple peaks (see SI. 2). Therefore, a PC:DDAB concentration ratio of 40:4.4 mM was selected as the preferred formulation, and subject to further investigations. Notably, the final lipid concentration under these operating conditions is significantly greater than the one used in most microfluidic reactors, and is within the typical range for medicinal products [23].

Additional experiments were subsequently carried out to investigate the effect of g-force on liposome dimensions. Consistently with the results reported above, the straight-RIAC produced liposomes with lower mean diameter (between 100 and 150 nm, Fig. 3C); nevertheless, liposome size dispersity was significantly greater compared to the spiral-RIAC (Fig. 3D). Liposome diameter didn't change significantly with varying the centrifugal force (in the range 447–1789 rcf), whilst liposome dispersity appeared to increase at rcf $> \sim 1'000$. As the liposome suspension exits the RIAC at greater velocity and travels towards the bottom of the centrifuge tube, it is likely subject to mechanical forces of greater magnitude (i.e.; in the form of shear or normal pressure forces). These may potentially cause some liposomes to rupture and/or aggregate, therefore impacting on liposomes size distribution.

Overall, operating the device at 447 rcf for 2 min (frit pore size = 2.0 μm) resulted in the highest reproducibility and the lowest liposome dispersity (PDI = 0.26), for the selected formulation of 40:4.4 mM PC:DDAB (Fig. 3 C,D).

3.3. Liposome production: Effect of the frit pore size

The effect of frit pore size (0.5 μm *vs.* 2.0 μm) was also investigated, using the spiral-RIAC and the selected lipid formulation (Fig. 4 A,B). Firstly, by comparing the results shown in Fig. 3C and 4A, which were obtained under the same operating conditions (see orange histograms), the high experimental reproducibility of RIAC's performance could be assessed. Moreover, RIACs having frits with different pore size produced liposomes with comparable mean diameter (Fig. 4A) and dispersity (Fig. 4B). The frit pore size however appeared to influence the reproducibility of the production method (see standard deviation of liposome mean diameter in Fig. 4A), with the 0.5 μm frit offering superior performance compared to the 2.0 μm frit (Fig. 4A). This observation could be due to differences in the hydraulic resistance offered by filters of different pore size, which may affect the velocity and temporal dynamics of the flow exiting both reservoirs. Further investigations are thus required to evaluate whether the presence of a frit filter may affect the flow dynamic field and mixing process within the reactor.

Finally, liposomal samples produced at 447 rcf were selected for TEM characterization (Fig. 4C), which confirmed that liposomes had a therapeutically viable diameter (i.e., < 230 nm).

3.4. Production of spherical silver nanoparticles (AgNPs)

In a second part of the study, the feasibility of using RIAC for inorganic synthesis was also evaluated, using the optimised operating parameters reported above. Spherical silver nanoparticles (AgNPs) were produced using the spiral-RIAC with 0.5 μm frit filters. AgNPs were synthesized by adapting a previous flow-synthesis protocol [13] based on the use of silver nitrate ($AgNO_3$), tri sodium citrate dehydrate (TSCD), polyvinylpyrrolidone (PVP), and sodium borohydride ($NaBH_4$) as reducing agent. AgNPs were characterised with UV–visible spectrophotometry and TEM. As shown in Fig. 5, nanoparticles had a clear absorption band due to surface plasmon resonance [32], with an absorption maxima (A_{max}) of 404 nm (Fig. 5A).

AgNP shape and size, as well as the uniformity of their size distribution, were also confirmed *via* TEM imaging (see wide-field image in Fig. 5B). The aim of these experiments was to provide a proof-of-concept demonstration of RIAC's utility for the production of metal nanoparticles. Additional studies should be carried out in the future to further optimise the operating conditions for these inorganic formulations, as well as explore potential effects of centrifugal forces on the size and shape of metal nanomaterials.

4. Conclusion

In this study, we introduced cost-effective, easy-to-use, and pump-free reactor-in-a-centrifuge (RIAC) devices. Depending on the architectural complexity, RIACs can be 3D printed in 4–6 h, at a bulk material (PLA) cost of ~£1.2 per device (considering an average cost of ~£0.04/g for a PLA filament, and 100% infill density), without the need for pre– or post–treatments. It is estimated that material costs are ~ 4.5-times lower than those associated with replica moulding methods based on 3D printed master moulds, as estimated previously [13]. Moreover, the proposed manufacturing method only requires a desktop 3D printer, which significantly reduces instrumentation-associated costs when compared to other replica moulding techniques relying on high-resolution 3D printing, micromilling, photolithography, and/or plasma bonding [33]. Importantly, it should be noted that the centrifuge-compatible RIAC architecture has been specifically conceived for manufacturing *via* cost-effective 3D printing, and it would be technically complex, time consuming, and/or expensive to manufacture with alternative (i.e., replica moulding) methods that are often employed to fabricate microfluidic-based flow reactors.

Notably, RIACs can be utilised and fabricated by users without prior expertise in flow-reactor manufacturing; concurrently, expert designers

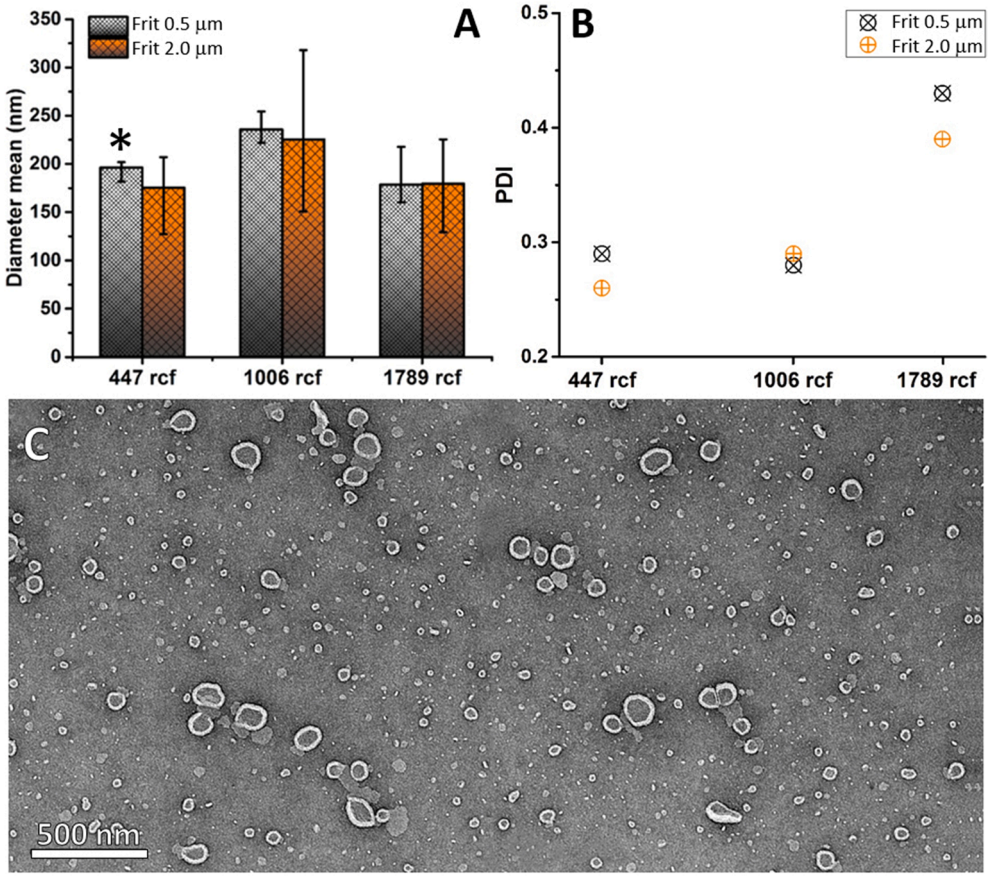

Fig. 4. Effect of frit pore size on the average diameter (A) and dispersity (B) of liposomes produced using the spiral-RIAC at different rcf values. (C) TEM images of two different areas of a representative sample (see * in A) produced under the following conditions: 2 mL of PC:DDAB 40:4.4 mM in EtOH (reservoir 1); 2 mL of water (reservoir 2); 6 mL of water at the bottom of the centrifuge tube; centrifuge parameters: 447 rcf for 2 min. Scale bar = 500 nm.

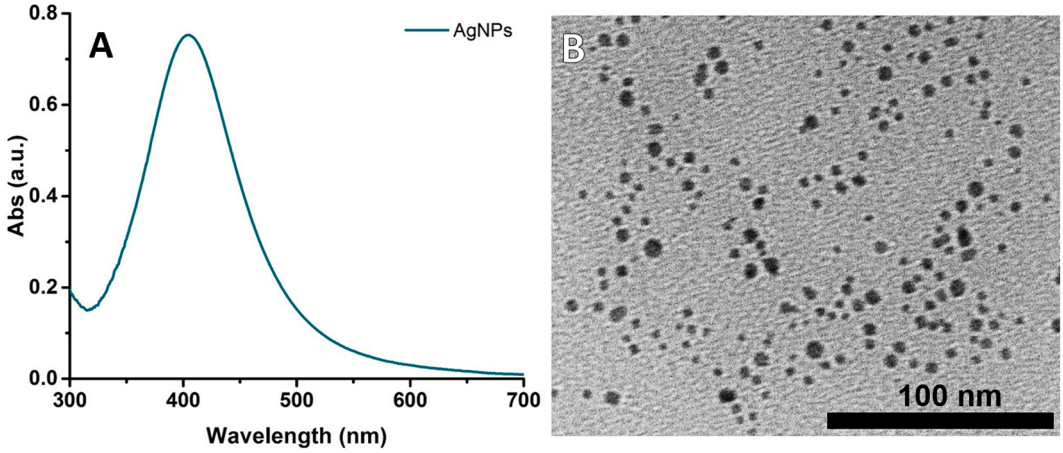

Fig. 5. (A) UV–vis spectrum of AgNPs showing the maximum surface plasmon resonance (SPR) absorption at 404 nm. (B) TEM of the same sample after a 1/3 dilution (scale bar = 100 nm).

have the flexibility to prototype architectures that best fit different applications. In this study, we reported on the manufacturing and testing of two different RIAC architectures, containing either a straight or spiral shaped mixing channel; these are channel configurations often employed in flow synthesis of nanoparticulate-based formulations. We demonstrated the use of these RIACs to produce size-controlled nanoscale liposomes, with a therapeutically relevant diameter < 230 nm, and we reported on the optimisation of the liposome production protocol. Additionally, we demonstrated the synthesis of metal nanomaterials (silver nanospheres) with typical structural and optical properties. Both particulate systems had dimensional properties that were comparable to the ones reported in previous studies using similar formulations [13,25]. To the best of the authors' knowledge, this is the first attempt at producing nanoscale vesicular systems and silver nanoparticles using a 3D printed flow-reactor that is solely driven by a conventional laboratory centrifuge. The developed technology could lead to the realization of a one-step synthesis/separation protocol for nanomaterials, where RIAC is employed simultaneously for synthesis and differential centrifugation of

the end-product [34]. The large parametric space offered by laboratory centrifuges (i.e. in terms of achievable centrifugal forces) may also enable greater mixing efficiencies compared to other flow reactor technologies based on pressure-driven flows. Moreover, given the high compatibility of PLA with multiple solvents, we envisage that RIACs could be applied to a number of different applications, including the rapid formulation and purification of drug-loaded nanoparticles, but also for performing chemical reactions by two-component mixing (notably, the system could be expanded to include an arbitrary number of reservoirs). Alternative constitutive materials may however be required for specific applications where PLA may not be chemically compatible. The availability of a bottom reservoir for reaction quenching and pre-purification further adds to the flexibility of the RIAC. As several RIACs can be employed in parallel, this approach may allow for rapid screening and optimisation of different reaction conditions. Depending on the required application, temperature-controlled and continuous-flow centrifuges may be also employed, both of which are commercially available or could be custom-made. Future research could investigate scaling-up strategies to achieve greater production rates and improve continuity of operation; these may require different solutions to those adopted for other types of pressure-driven flow reactors. Potential approaches may rely on increasing the overall dimensions of the reactor, simultaneously operating multiple devices, and/or automating the reactor priming and sample collection processes. Moreover, the RIAC architecture has been specifically conceived to enable cost-effective and rapid manufacturing, which also makes the reactor itself economically viable for scaling-up. As for other flow reactor technologies, any identified scaling-up strategy will however require a full assessment of associated costs and technological complexities, relative to the corresponding production rates.

Future work may also focus on performing an accurate quantitative evaluation of the residence time of chemical species within the RIAC, i.e. using numerical models, which could then be tuned to meet reaction-specific requirements. Finally, additional experiments could be performed to fully assess the potential of centrifugal forces as a means to tune the size and shape of metal nanoparticles.

Declaration of Competing Interest

The authors declare that they have no known competing financial interests or personal relationships that could have appeared to influence the work reported in this paper.

Acknowledgments

The authors would like to thank the Engineering and Physical Sciences Research Council (EPSRC) for supporting the research presented in this paper. Andrea Cristaldi's PhD studentship was funded by an EPSRC Doctoral Training Partnerships (DTP) scheme at the University of Southampton.

Appendix A. Supplementary data

Supplementary data to this article can be found online at https://doi.org/10.1016/j.cej.2021.130656.

References

[1] F.M. Akwi, P. Watts, Continuous flow chemistry: where are we now? Recent applications, challenges and limitations, Chem. Communications 54 (99) (2018) 13894–13928.
[2] B.K. Gale, A.R. Jafek, C.J. Lambert, B.L. Goenner, H. Moghimifam, U.C. Nze, S. K. Kamarapu, A review of current methods in microfluidic device fabrication and future commercialization prospects, Inventions 3 (3) (2018) 60.
[3] K.S. Elvira, X.C. i Solvas, R.C.R. Wootton, A.J. deMello, The past, present and potential for microfluidic reactor technology in chemical synthesis, Nat. Chem. 5 (11) (2013) 905–915.
[4] D. van Swaay, A. DeMello, Microfluidic methods for forming liposomes, Lab Chip 13 (5) (2013) 752–767.
[5] R.R. Hood, D.L. DeVoe, High-throughput continuous flow production of nanoscale liposomes by microfluidic vertical flow focusing, small 11 (43) (2015) 5790–5799.
[6] N. Hao, Y. Nie, J.X.J. Zhang, Microfluidic synthesis of functional inorganic micro-/nanoparticles and applications in biomedical engineering, Int. Mater. Rev. 63 (8) (2018) 461–487.
[7] G.M. Whitesides, E. Ostuni, S. Takayama, X. Jiang, D.E. Ingber, Soft lithography in biology and biochemistry, Annu. Rev. Biomed. Eng. 3 (1) (2001) 335–373.
[8] H.N. Chan, Y. Chen, Y. Shu, Y. Chen, Q. Tian, H. Wu, Direct, one-step molding of 3D-printed structures for convenient fabrication of truly 3D PDMS microfluidic chips, Microfluid. Nanofluid. 19 (1) (2015) 9–18.
[9] Z. Chen, J.Y. Han, L. Shumate, R. Fedak, D.L. DeVoe, High throughput nanoliposome formation using 3D printed microfluidic flow focusing chips, Adv. Mater. Technologies 4 (6) (2019) 1800511, https://doi.org/10.1002/admt.v4.610.1002/admt.201800511.
[10] G. Comina, A. Suska, D. Filippini, PDMS lab-on-a-chip fabrication using 3D printed templates, Lab Chip 14 (2) (2014) 424–430.
[11] H. Gong, B.P. Bickham, A.T. Woolley, G.P. Nordin, Custom 3D printer and resin for 18 μm×20 μm microfluidic flow channels, Lab Chip 17 (17) (2017) 2899–2909.
[12] D. Carugo, J.Y. Lee, A. Pora, R.J. Browning, L. Capretto, C. Nastruzzi, E. Stride, Facile and cost-effective production of microscale PDMS architectures using a combined micromilling-replica moulding (μMi-REM) technique, Biomed. Microdevices 18 (1) (2016) 4.
[13] D.A. Cristaldi, F. Yanar, A. Mosayyebi, P. García-Manrique, E. Stulz, D. Carugo, X. Zhang, Easy-to-perform and cost-effective fabrication of continuous-flow reactors and their application for nanomaterials synthesis, New Biotechnol. 47 (2018) 1–7.
[14] E. Amstad, X. Chen, M. Eggersdorfer, N. Cohen, T.E. Kodger, C.L. Ren, D.A. Weitz, Parallelization of microfluidic flow-focusing devices, Phys. Rev. E 95 (4) (2017), 043105.
[15] M. Madou, J. Zoval, G. Jia, H. Kido, J. Kim, N. Kim, Lab on a CD, Annu. Rev. Biomed. Eng. 8 (1) (2006) 601–628.
[16] L.X. Kong, A. Perebikovsky, J. Moebius, L. Kulinsky, M. Madou, Lab-on-a-CD: A fully integrated molecular diagnostic system, J. Lab. Automation 21 (3) (2016) 323–355.
[17] E. Roy, G. Stewart, M. Mounier, L. Malic, R. Peytavi, L. Clime, M. Madou, M. Bossinot, M.G. Bergeron, T. Veres, From cellular lysis to microarray detection, an integrated thermoplastic elastomer (TPE) point of care lab on a disc, Lab Chip 15 (2) (2015) 406–416.
[18] A. Kloke, A.R. Fiebach, S. Zhang, L. Drechsel, S. Niekrawietz, M.M. Hoehl, R. Kneusel, K. Panthel, J. Steigert, F. von Stetten, R. Zengerle, N. Paust, The LabTube–a novel microfluidic platform for assay automation in laboratory centrifuges, Lab Chip 14 (9) (2014) 1527–1537.
[19] M.M. Hoehl, E.S. Bocholt, A. Kloke, N. Paust, F.V. Stetten, R. Zengerle, J. Steigert, A.H. Slocum, A versatile-deployable bacterial detection system for food and environmental safety based on LabTube-automated DNA purification LabReader-integrated amplification, readout and analysis, Analyst 139 (11) (2014) 2788–2798.
[20] H. Daraee, A. Etemadi, M. Kouhi, S. Alimirzalu, A. Akbarzadeh, Application of liposomes in medicine and drug delivery, Artif. Cells Nanomed. Biotechnol. 44 (1) (2016) 381–391.
[21] A. Panáček, L. Kvitek, R. Prucek, M. Kolář, R. Večeřová, N. Pizúrová, V.K. Sharma, T.j. Nevěčná, R. Zbořil, Silver colloid nanoparticles: synthesis, characterization, and their antibacterial activity, The Journal of Physical Chemistry B 110(33) (2006) 16248-16253.
[22] Susanne Schweiger, Alois Jungbauer, Scalability of pre-packed preparative chromatography columns with different diameters and lengths taking into account extra column effects, J. Chromatogr. A 1537 (2018) 66–74.
[23] D. Carugo, E. Bottaro, J. Owen, E. Stride, C. Nastruzzi, Liposome production by microfluidics: potential and limiting factors, Sci. Rep. 6 (1) (2016) 1–15.
[24] L. Capretto, D. Carugo, S. Mazzitelli, C. Nastruzzi, X. Zhang, Microfluidic and lab-on-a-chip preparation routes for organic nanoparticles and vesicular systems for nanomedicine applications, Adv. Drug Deliv. Rev. 65 (11-12) (2013) 1496–1532.
[25] F. Yanar, A. Mosayyebi, C. Nastruzzi, D. Carugo, X. Zhang, Continuous-Flow Production of Liposomes with a Millireactor under Varying Fluidic Conditions, Pharmaceutics 12 (11) (2020) 1001.
[26] M. Carboni, L. Capretto, D. Carugo, E. Stulz, X. Zhang, Microfluidics-based continuous flow formation of triangular silver nanoprisms with tuneable surface plasmon resonance, J. Mater. Chem. C 1 (45) (2013) 7540–7546.
[27] M.J. Kennedy, H.D. Ladouceur, T. Moeller, D. Kirui, C.A. Batt, Analysis of a laminar-flow diffusional mixer for directed self-assembly of liposomes, Biomicrofluidics 6 (4) (2012) 044119, https://doi.org/10.1063/1.4772602.
[28] N. Nivedita, P. Ligrani, I. Papautsky, Dean flow dynamics in low-aspect ratio spiral microchannels, Sci. Rep. 7 (1) (2017) 1–10.
[29] M.K. Verma, S.R. Ganneboyina, R. Vinayak Rakshith, A. Ghatak, Three-dimensional multihelical microfluidic mixers for rapid mixing of liquids, Langmuir 24 (5) (2008) 2248–2251.
[30] C.-Y. Lee, W.-T. Wang, C.-C. Liu, L.-M. Fu, Passive mixers in microfluidic systems: a review, Chem. Eng. J. 288 (2016) 146–160.
[31] E. Bottaro, A. Mosayyebi, D. Carugo, C. Nastruzzi, Analysis of the diffusion process by pH indicator in microfluidic chips for liposome production, Micromachines 8 (7) (2017) 209.

[32] D. Paramelle, A. Sadovoy, S. Gorelik, P. Free, J. Hobley, D.G. Fernig, A rapid method to estimate the concentration of citrate capped silver nanoparticles from UV-visible light spectra, Analyst 139 (19) (2014) 4855–4861.
[33] S.K. Tiwari, S. Bhat, K.K. Mahato, Design and fabrication of low-cost microfluidic channel for biomedical application, Sci. Rep. 10 (1) (2020) 1–14.
[34] A.K. Suresh, D.A. Pelletier, J.W. Moon, T. Phelps, M.J. Doktycz, Size-separation of silver nanoparticles using sucrose gradient centrifugation, J. Chromatogr. Sep. Tech. 6 (5) (2015).